4.3 INTERCOMPARISON OF GLOBAL UPPER-AIR TEMPERATURE DATASETS FROM RADIOSONDES AND SATELLITES

D.J. Seidel[1], J. Angell[1], J. Christy[2], M. Free[1], S. Klein[3], J. Lanzante[3], C. Mears[4], D. Parker[5], M. Schabel[4], R. Spencer[2], A. Sterin[6], P. Thorne[5], and F. Wentz[4]

[1]NOAA Air Resources Laboratory, Silver Spring, Maryland
[2]University of Alabama in Huntsville, Huntsville, Alabama
[3]NOAA Geophysical Fluid Dynamics Laboratory, Princeton, New Jersey
[4]Remote Sensing Systems, Santa Rosa, California
[5]Met Office, Bracknell, Berkshire, United Kingdom
[6]All-Russian Research Institute of Hydrometeorological Information, Obninsk, Kaluga Region, Russian Federation

1. INTRODUCTION

Global upper-air temperature datasets figure prominently in climate change detection and attribution studies. Radiosonde and satellite observations have been compiled to create long-term datasets for climate studies. Different groups have addressed data quality, spatial sampling, and temporal homogeneity issues differently, and no single data product has yet emerged as a generally-recognized reference. Thus a suite of datasets is available to the scientific community, and differences among them are a measure of our uncertainty about changes in upper-air temperature over the past two to five decades.

Here we present some results from an intercomparison of eight datasets produced by six research groups. Previous intercomparisons (Hurrell and Trenberth, 1998; Santer et al., 1999, 2000; Gaffen et al., 2000; NRC, 2000; Hurrell et al., 2000, Ramaswamy et al., 2001), including those made for the Intergovernmental Panel on Climate Change (IPCC) assessment reports, have examined fewer datasets and have focused on temperature trends (particularly in the lower troposphere and at the surface), global sampling issues, and the utility of reanalysis data products. We extend these studies by incorporating new datasets and examining other statistical measures of variability as well as trends, with a goal of better characterizing the uncertainty of observational estimates of upper-air temperature change.

2. DATASETS

The following datasets are included in our intercomparison. Each has been (or will soon be) presented in peer-reviewed journals and most have figured in IPCC assessment reports. We include three datasets based on the Microwave Sounding Unit (MSU, and the Advanced MSU) that has flown on NOAA polar-orbiting satellites since 1979 and five datasets based on subsets of the global radiosonde data archive. Basic features of these eight datasets are as follows.

2.1 *Satellite MSU Datasets*

UAH-MSU ver. D - Monthly, gridded, global temperature anomalies for 1979-2001for the lower stratosphere (MSU-4), troposphere (MSU-2), and lower troposphere (MSU-2LT). Quality control and procedures for merging data from different satellites are described by Christy et al. (2000). Version D was the fourth to be made publicly available by John Christy and Roy Spencer of the University of Alabama in Huntsville (UAH).

UAH-MSU ver. 5 - A more recent update of the previous dataset, with a different (nonlinear rather than linear) correction for time-varying sampling of the diurnal cycle by the MSU instruments (Christy et al., submitted). This difference applies to MSU-2 and MSU-2LT, but not to MSU-4, which is identical in versions D and 5.

RSS-MSU - Monthly, gridded, global temperature anomalies for 1979-2001 for the lower stratosphere (MSU-4), tropopause region (MSU-3) and troposphere (MSU-2). The dataset is produced by Frank Wentz, Carl Mears, and Matthias Schabel of Remote Sensing Systems, Inc. (RSS) using different corrections and merging procedures than used by UAH (Mears et al., submitted).

2.2 *Radiosonde Datasets*

Angell-63 - Global, hemispheric, and zonal seasonal temperature anomalies for 1958-2001 in three pressure layers (850-300 hPa, 300-100 hPa, and 100-50 hPa), based on daily sounding data from a 63-station network. No adjustments for data inhomogeneities are made. Details are described by Angell (1988) and references therein. The dataset is prduced by Jim Angell at the NOAA Air Resources Laboratory.

*Corresponding author address: Dian Seidel, NOAA R/ARL, 1315 East West Hwy., Silver Spring, MD 20910; E-mail: dian.seidel@noaa.gov

Angell-54 - A recent revision of Angell-63 in which nine tropical radiosonde stations, whose stratospheric temperature trends were highly anomalous, were removed from the network (Angell, submitted).

HadRT - Monthly, gridded, global temperature anomalies based on data from radiosonde stations providing monthly temperature (CLIMAT TEMP) reports. Data for 1958-2001 are available at nine pressure levels between 850 and 30 hPa. Stratospheric data since 1979 have been adjusted using UAH-MSU ver. D. The adjustments are spatially patchy because they were made only if significant temperature changes were accompanied by known station history events. This is HadRT2.1s as described by Parker et al. (1997) and was prepared by David Parker, Margaret Gordon, and Peter Thorne of the UK Met Office's Hadley Centre for Climate Prediction and Research.

LKS - A new monthly global temperature anomaly dataset based on data from 87 radiosonde stations and incorporating temporal homogeneity adjustments that are independent of other upper-air temperature datasets. The adjustments are based on a suite of indicators, including day-night temperature differences, the vertical structure of temperature, station history information, statistical measures of abrupt change, and indices of real climate variations. Data are available at the surface and 15 pressure levels from 1000 to 10 hPa. The dataset is described by Lanzante et al. (to appear) and prepared by John **L**anzante and Steve **K**lein (NOAA Geophysical Fluid Dynamics Lab) and Dian **S**eidel (NOAA Air Resources Lab).

RIHMI - Monthly, global gridded temperature anomalies from the global radiosonde network. Spatial interpolation fills data-void regions. Prepared by Alex Sterin at the All-Russian Research Institute of Hydrometeorological Information and described by Sterin (1999). For this study data for two layers (850-300 hPa and 100-50 hPa) were available.

3. TIME SERIES

To facilitate the intercomparison, temperature anomaly time series were prepared for each dataset in four regions and for a subset of 23 vertical levels and layers. The regions are: Globe, Northern Hemisphere (equator-90N), Southern Hemisphere (equator-90S), and Tropics (30N-30S). The levels and layers include the surface, 15 pressure levels, the three layers defined by Angell (1988 - see Angell-63 above), and four MSU layers (2, 2LT, 3, and 4 - see UAH-MSU and RSS-MSU above).

Weighting functions were applied to pressure level radiosonde data from HadRT and LKS to simulate the MSU and Angell layers. Intercomparisons shown here are for two periods: 1958-1997 for the five radiosonde datasets and 1979-2001 for the satellite and radiosonde datasets (excluding LKS, which ends in 1997).

Here we focus on the global monthly temperature anomaly time series for the MSU layers 2, 2LT and 4 and for the three pressure layers defined by Angell (1988). Figures 1-5 show data for five of these layers, with the bottom curves in each figure showing the average of all available datasets and the other curves showing departures of individual time series from this multi-dataset average. The curves have been shifted by an additive constant for plotting. The following sections discuss statistical aspects of the time series from which Figures 1-5 are derived and similar time series for the hemispheres and for the tropics.

Without attempting a detailed discussion of these plots, we point out the following features which are visually apparent in these time series:

- The global tropospheric temperature anomaly datasets (Figs. 1, 3, and 4) show, in the average (AVG) curves, warming of the troposphere that is not monotonic but has considerable variability on monthly, interannual, and interdecadal time scales.

- The global stratospheric anomaly time series (Figs. 2 and 5), in the AVG curves, show evidence of stratospheric cooling, which is also not monotonic. Strong transient warming episodes are apparent in the early 1960's, early 1980's, and early 1990's associated with volcanic eruptions.

- The differences between individual datasets and the AVG curves in Figs. 1-5 are not simply random noise. The difference curves have step-like changes, long-term trends, and interannual signals.

4. VARIABILITY

Figure 6 presents a simple comparison of the variability of the global monthly anomaly time series for 1979-1997, the period covered by all the datasets. The standard deviations of the radiosonde time series are shown on the left panel, and those for the satellite and radisonde-simulated satellite datasets are on the right panel. Note the larger standard deviations in the stratosphere (100-50 hPa and MSU4 layers) than in the troposphere.

The variability of most of the datasets is comparable for a given layer, with the exception of RIHMI, which has markedly smaller standard deviations. Note the slightly greater variability of the Angell datasets compared with the other radiosonde datasets, which is likely due to the

more limited station network used by Angell. The reduction in variability from Angell-63 to Angell-54 is associated with the removal of outlier stations in the latter dataset.

5. AUTOCORRELATION

Lag-one autocorrelations (not shown) of these global anomaly time series vary between ~0.5 in the troposphere and ~0.9 in the stratosphere. The high autocorrelation in the stratosphere is associated with the strong downward temperature trend. The Angell datasets have anomalously high autocorrelation because they are based on seasonal, not monthly, data. The radiosonde-simulated MSU layer time series have somewhat lower autocorrelation than the actual MSU time series.

6. LINEAR TRENDS

Linear temperature trends are shown in Figs. 7 and 8 for the radiosonde and MSU layers, respectively. Each figure shows trends for the globe, Northern and Southern Hemispheres, and tropics. In examining these linear trends, recall that the time series show considerable variability that is neither trend-like nor linear in nature.

The radiosonde-layer trends (Fig. 7) are for 1958-1997 and show warming in the 850-300 hPa layer and cooling in the 100-50 hPa layer. The magnitudes of these trends vary markedly, with statistically significantly different trends in almost all the regions and layers. Consistent with their lower variability, the RIMHI data have lower trends. The trends are somewhat more consistent in the Northern Hemisphere than in the Southern, probably reflecting the relatively better sampling of the Northern Hemisphere by each radiosonde dataset. In the 300-100 hPa layer there is little agreement among the datasets, particularly in the tropics, where the sign of the trend seems highly uncertain.

The satellite-layer trends (Fig. 8) are for 1979-2001. In the stratosphere (MSU4), trends from the RSS and two UAH datasets are in relatively good agreement, but are much smaller than the trends in the HadRT data simulating MSU 4. Although the HadRT dataset appears to be an outlier in Fig. 8, this is somewhat misleading. For the shorter period 1979-1997, trends in the MSU4 layer derived from LKS data are closer to the HadRT values than to either the RSS or UAH results. And lower stratospheric (100-50 hPa) trends from both Angell-63 and Angell-54 (but not from RIMHI) are also larger than the MSU-4 trends, suggesting that radiosonde datasets, in general, show more stratospheric cooling than do satellite datasets.

In the troposphere (MSU2) and lower troposphere (MSU2LT) there are small but noticeable differences between the two versions of the UAH data. The MSU2 data from RSS show stronger upward temperature trends than either UAH version, but the differences are generally not statistically significant. The HadRT data for the MSU2 layer indicate tropospheric cooling.

7. CROSS-CORRELATIONS

Correlations among the time series are shown in Tables 1, 2 and 3. Table 1 addresses global radiosonde datasets for 1958-1997, Table 2 addresses global MSU datasets and radiosonde-simulated MSU for 1979-1997, and Table 3 compares the Northern and Southern Hemisphere correlations for the MSU2 layer.

Table 1 shows that the radiosonde datasets are better correlated for the 850-300 and 100-50 hPa layers than for the 300-100 hPa layer. Correlations range from ~0.5 to ~0.9.

Table 2 shows that the UAH version D, UAH version 5, and RSS versions of MSU4 and MSU2 are highly correlated (0.92 to 0.98), as are the two versions of MSU2LT from UAH. The radiosonde-simulated MSU layer time series show lower correlations with the actual MSU data than the correlations between MSU products.

Table 2 also indicates that, compared with the HadRT data, the LKS data are more highly correlated with MSU4, MSU2, and MSU2LT data from either UAH version, or from RSS. This is somewhat surprising because the HadRT stratospheric data from some stations are adjusted to the UAH-MSU ver.D data and the LKS data are independently adjusted. On the other hand, the vertical resolution of the HadRT dataset is not as fine as the LKS dataset, which may affect the simulation of the MSU layers, particularly MSU2LT (because HadRT's lowest level is at 850 hPa).

The correlations for MSU2 are systematically higher for the Northern Hemisphere than the Southern Hemisphere, as shown in Table 3. This is expected for the radiosonde data, which sample the Northern Hemisphere better, but is also true for the correlations among the two UAH and the RSS datasets, which sample both hemispheres similarly.

9. FUTURE WORK

Further analysis of these data will involve a more comprehensive set of regions and vertical layers to highlight areas of enhanced or reduced uncertainty. We

also intend to include new versions of at least two of the datasets shown here. The RIHMI dataset is currently being revised based, in part, on the results of this study. The LKS dataset is being extended (from 1997 to present) and expanded to include more stations (for improved spatial representation) to form a new NOAA Radiosonde Atmospheric Temperature Products for Assessing Climate (RATPAC).

Acknowledgments: We thank Roland Draxler and Julian Wang (NOAA Air Resources Laboratory) for helpful comments. David Parker and Peter Thorne are supported by the U.K. Government Meteorological Research Programme and by the U.K. Dept. of Environment, Food and Rural Affairs contract PECD7/12/37.

REFERENCES

Angell, J.K., 1988: Variations and trends in tropospheric and stratospheric global temperatures, 1958-87, *J. Climate*, **1**, 1296-1313.

Angell, J.K., Effect of exclusion of anomalous tropical stations on tropical, hemispheric and global temperature trends from a 63-station radiosonde network, 1958-2000 and 1979-2000, and comparison with MSU and other radiosonde trends. Submitted to *J. Climate*.

Christy, J.R., R.W. Spencer, and W.D. Braswell, 2000: MSU Tropospheric temperatures: Data set construction and radiosonde comparisons. *J. Atmos. Oceanic Tech*., **17**,1153-1170.

Christy, J.R., R.W. Spencer, W.B. Norris, W.D. Braswell and D.E. Parker, Error estimates of Version 5.0 of MSU/AMSU bulk atmospheric temperatures. Submitted to *J. Atmos. Oc. Tech*.

Gaffen, D.J., M.A. Sargent, R.E. Habermann, and J.R. Lanzante, 2000: Sensitivity of tropospheric and stratospheric temperature trends to radiosonde data quality. *J. Climate*, **13**, 1776-1796.

Hurrell, J.W., and K.E. Trenberth, 1998: Difficulties in obtaining reliable temperature trends: Reconciling the surface and satellite microwave sounding unit records. *J. Climate,* **11**, 945-967.

Hurrell, J.W., S.J. Brown, K.E. Trenberth, J.R. Christy, 2000: Comparison of tropospheric temperatures from radiosondes and satellites: 1979-98. *Bull. Amer. Meteor. Soc*., **81**, 2165-2178.

Lanzante, J.R., S.A. Klein, and D.J. Seidel, Temporal homogenization of monthly radiosonde temperature data. Part I: Methodology. *J. Climate,* to appear.

Lanzante, J.R., S.A. Klein, and D.J. Seidel, Temporal homogenization of monthly radiosonde temperature data. Part II: Trends, sensitivities, and MSU comparison. *J. Climate*, to appear.

Mears, C.A., M.C Schabel, and F.J. Wentz, A reanalysis of the MSU channel 2 tropospheric temperature record. Submitted to *J. Climate*.

National Research Council (NRC), 2000: *Reconciling Observations of Global Temperature Change*, National Academy Press, Washington, DC, 85 pp.

Parker, D.E., M. Gordon, D.P.N. Cullum, D.M.H. Sexton, C.K. Folland, and N. Rayner 1997: A new global gridded radiosonde temperature data base and recent temperature trends. *Geophys. Res. Lett.,* **24**, 1499-1502.

Ramaswamy, V., M.-L. Chanin, J. Angell, J. Barnett, D. Gaffen, M. Gelman, P. Kekhut, Y. Koshelkov, K. Labitzke, J.-J. R. Lin, A. O'Neill, J. Nash, W. Randel, R. Rood, K. Shine, M. Shiotani, and R. Swinbank, 2001: Stratospheric temperature trends: Observations and model simulations. *Rev. Geophys*., **39**, 71-122.

Santer. B.D., J.J. Hnilo, T.M.L. Wigley, J.S. Boyle, C. Doutriaux, M. Fiorino, D.E. Parker, and K.E. Taylor, 1999: Uncertainties in observationally based estimates of temperature change in the free atmosphere. *J. Geophys. Res.,* **104**, 6305-6333.

Santer, B.D., T.M.L. Wigley, J.S. Boyle, D.J. Gaffen, J.J. Hnilo, D. Nychka, D.E. Parker and K.E. Taylor, 2000: Statistical significance of trend differences in layer-average temperature time series. *J. Geophys. Res.*, **105**, 7337-7356.

Sterin, A.M., 1999: An analysis of linear trends in the free atmosphere temperature series for 1958-1997. *Meteorologiai Gidrologia*, **5**, 52-68.

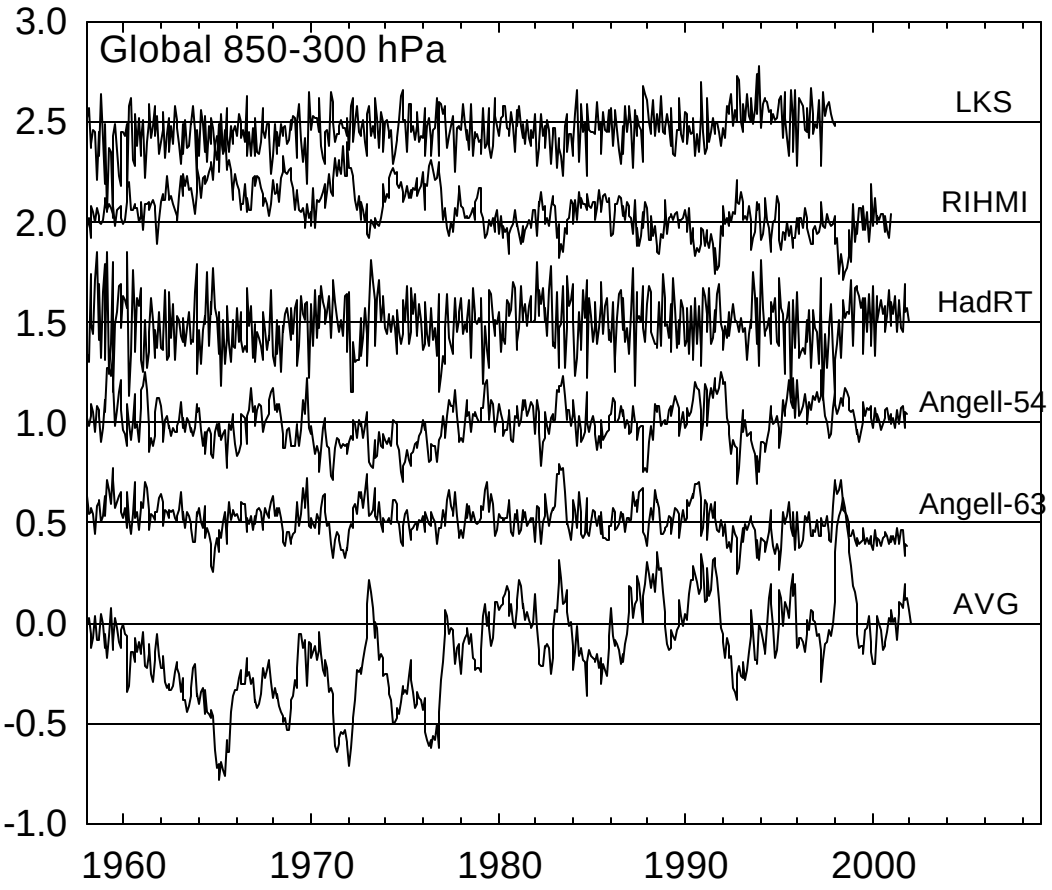

Figure 1. Global temperature anomalies (K) in the 850-300 hPa layer from five radiosonde datasets. The bottom curve is the average of the five, and the other curves show deviations from this five-dataset average. The curves have been shifted by an additive constant for plotting. LKS, RIHMI, and HadRT data are monthly; Angell-63 and Angell-54 data are seasonal.

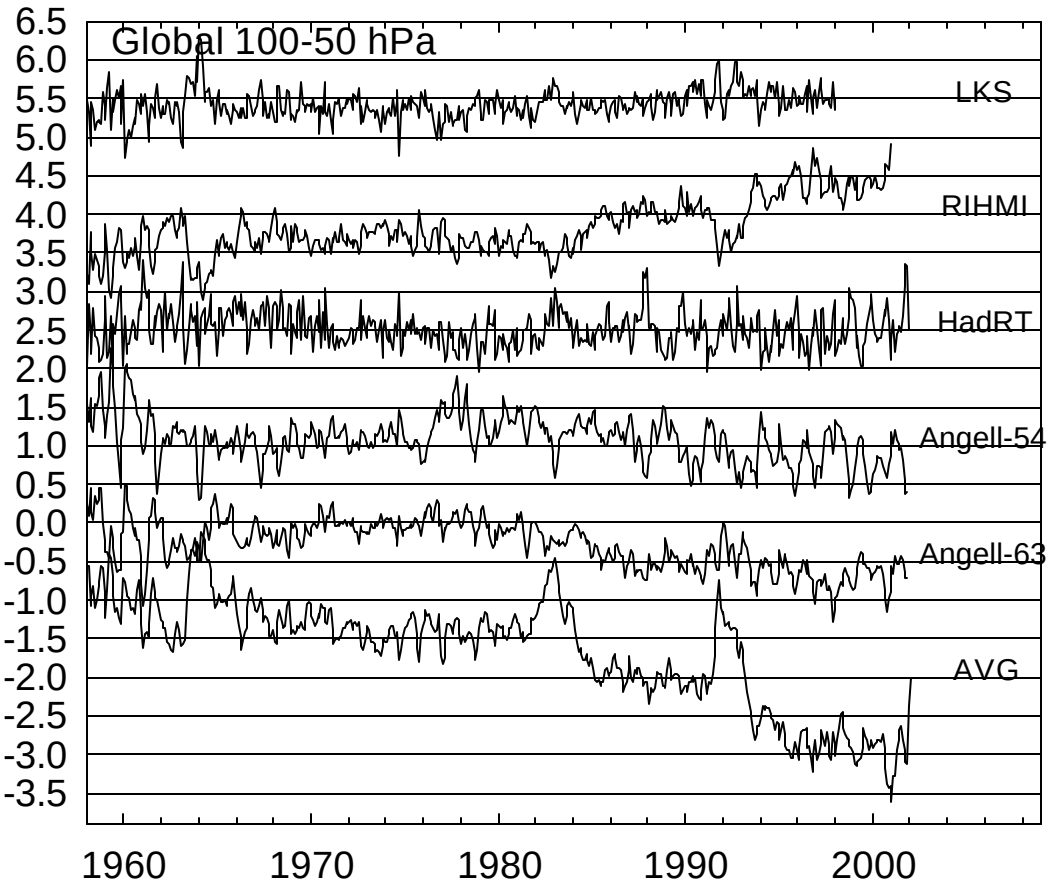

Figure 2. Global temperature anomalies (K) in the 100-50 hPa layer from five radiosonde datasets. The bottom curve is the average of the five, and the other curves show deviations from the five-dataset average. The curves have been shifted by an additive constant for plotting. LKS, RIHMI, and HadRT data are monthly; Angell-63 and Angell-54 data are seasonal.

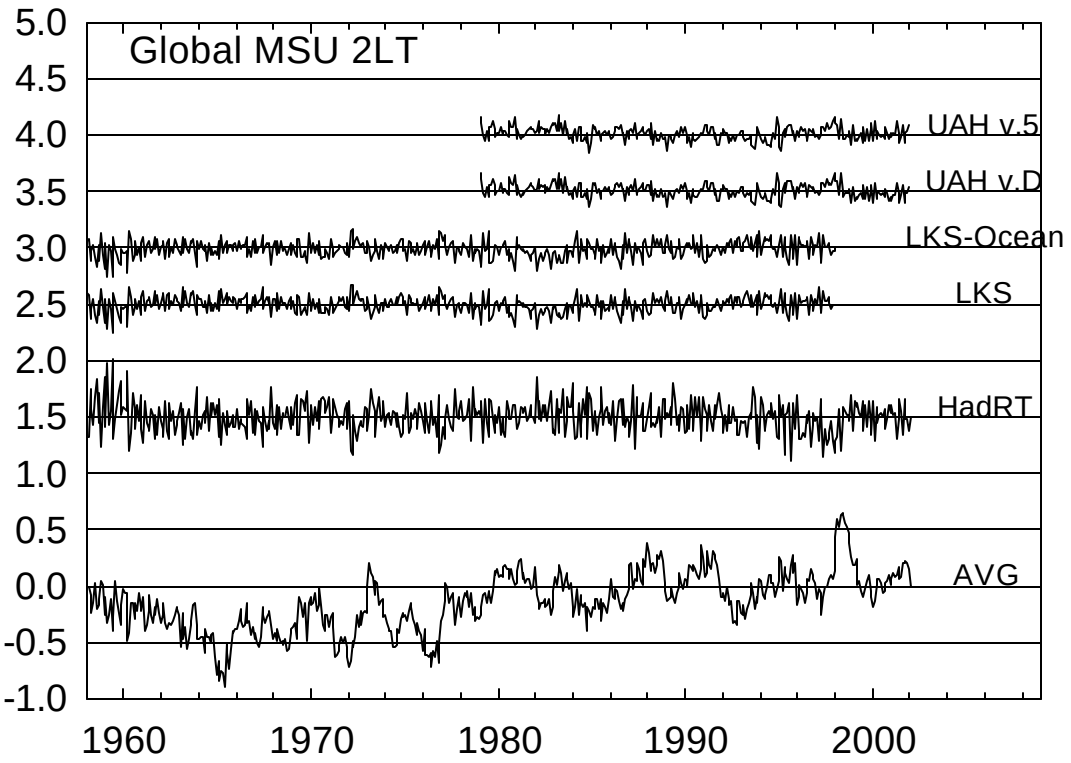

Figure 3. Global temperature anomalies (K) in the MSU 2LT layer (lower troposphere) from two UAH-MSU datasets and (simulated) from two radiosonde datasets. Two weighting functions (one for ocean and one for land) were applied to the LKS data, but the differences were negligible. The bottom curve is the average of the five, and the other curves show deviations from the average. The curves have been shifted by an additive constant for plotting.

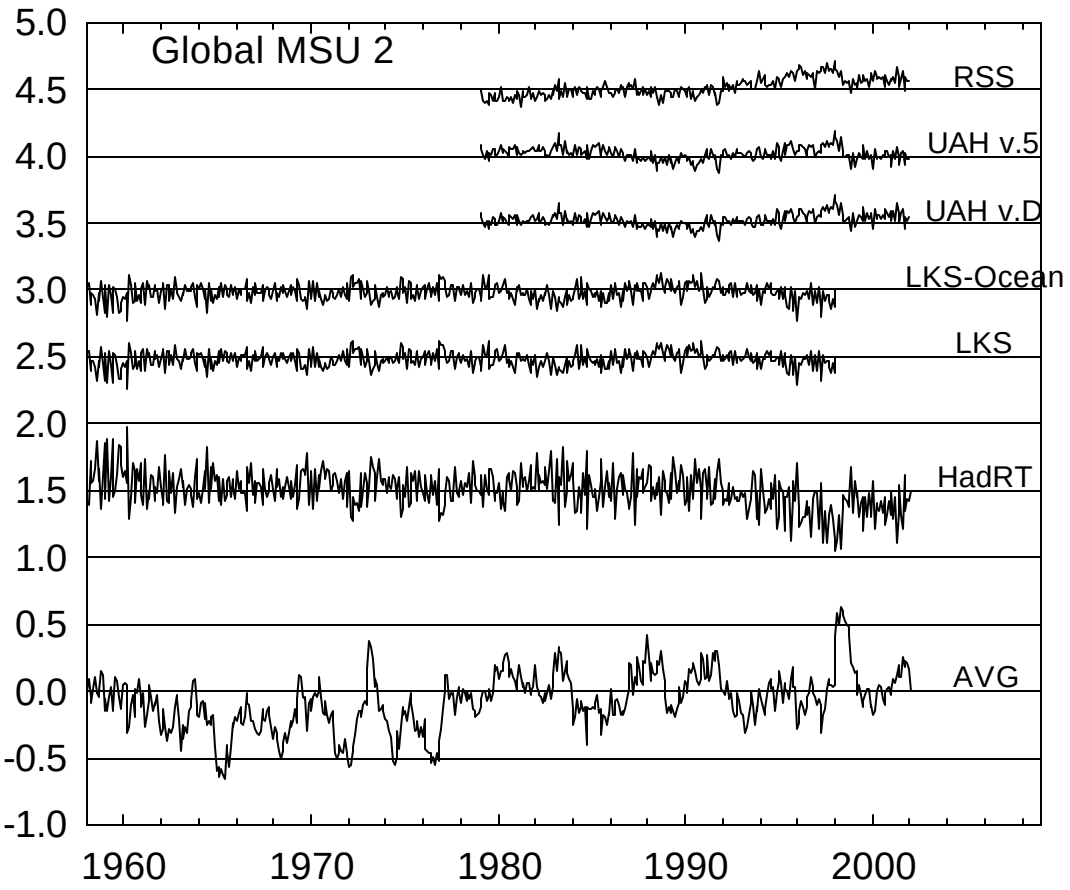

Figure 4. Global temperature anomalies (K) in the MSU 2 layer (troposphere) from two UAH-MSU datasets, the RSS-MSU dataset and (simulated) from two radiosonde datasets. As in Figure 3, two weighting functions were applied to the LKS data, with negligible differences resulting. The bottom curve is the average of the five, and the other curves show deviations from the average. The curves have been shifted by an additive constant for plotting.

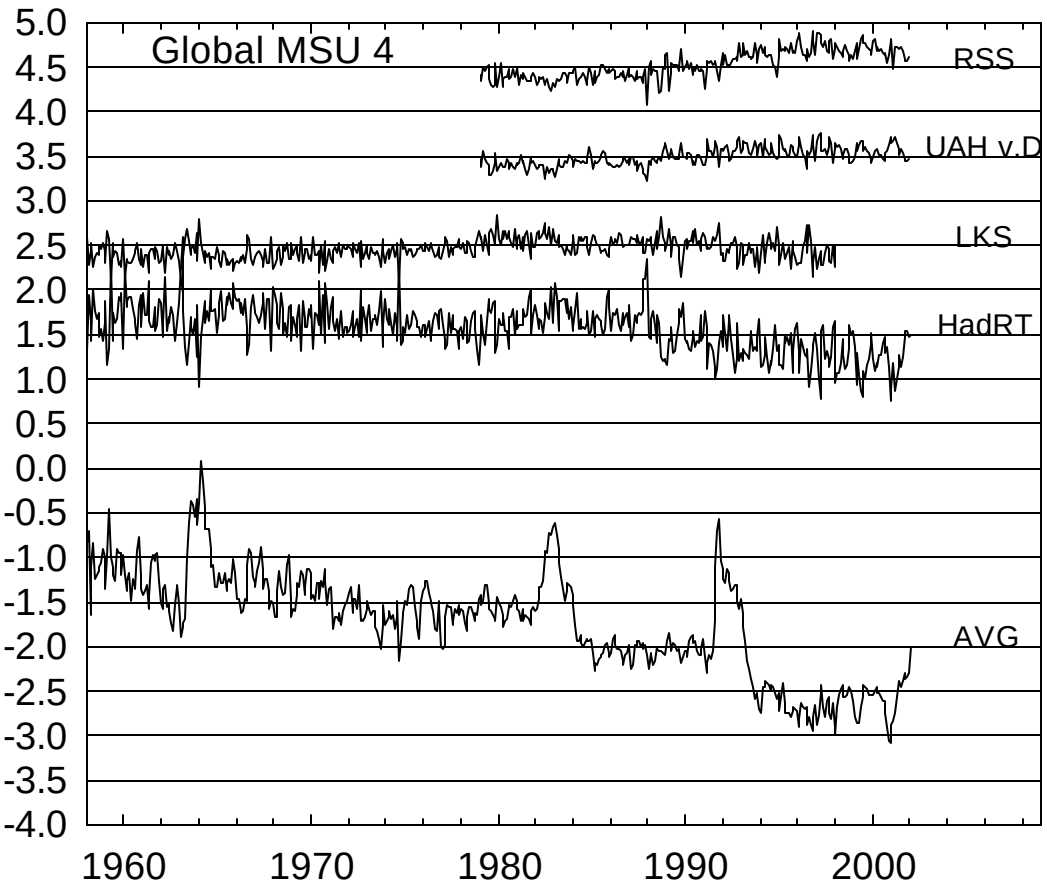

Figure 5. Global temperature anomalies (K) in the MSU 4 layer (lower stratoposphere) from the UAH-MSU and the RSS-MSU dataset and (simulated) from two radiosonde datasets. UAH-MSU ver.D and ver.5 are identical for this layer and so only one is shown. The bottom curve is the average of the four, and the other curves show deviations from the average. The curves have been shifted by an additive constant for plotting.

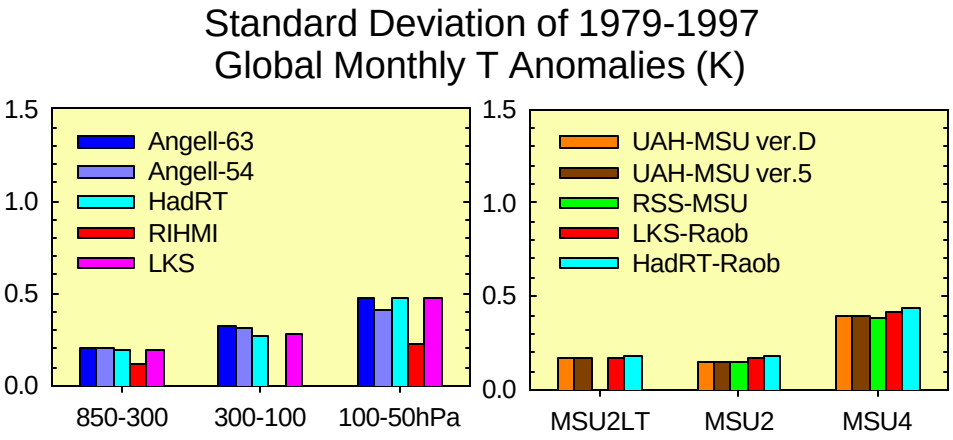

Figure 6. Standard deviations (K) of 1979-1997 global temperature anomalies (K) for the 3 radiosonde and 3 MSU layers shown.

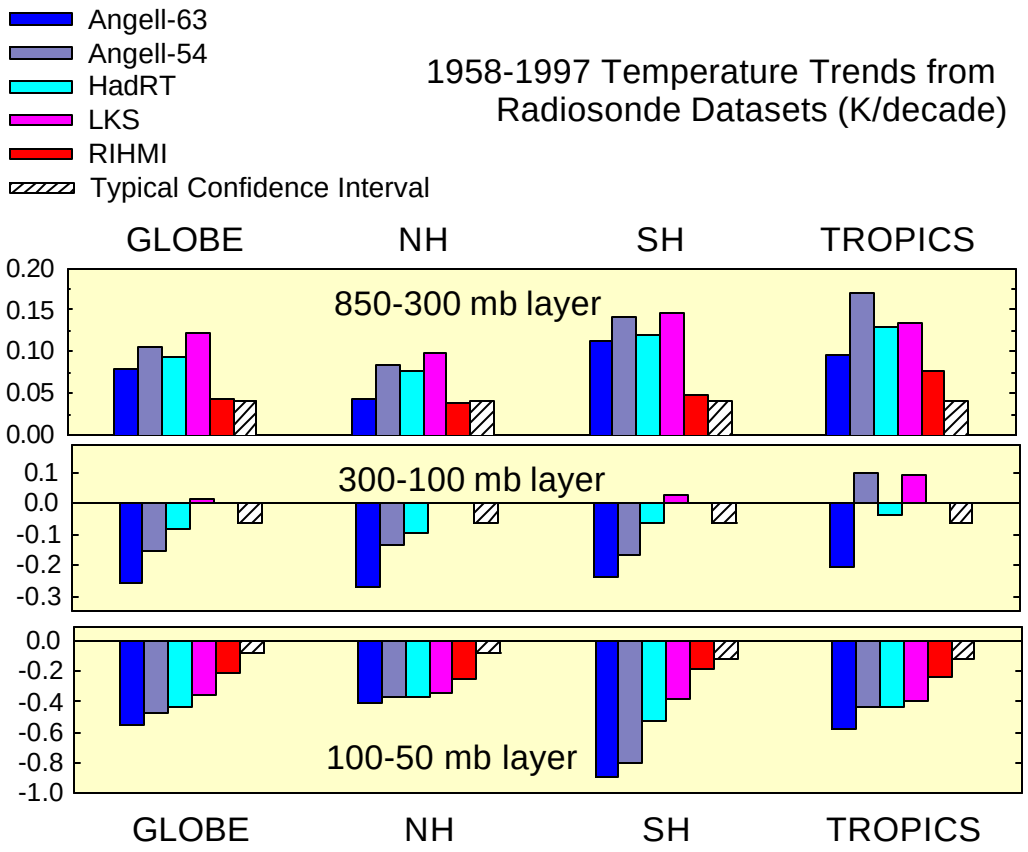

Figure 7. Trends in global temperature for 1958-1997 for three vertical layers, in four regions, from radiosonde datasets. The confidence intervals shown are typical values of the ±2 sigma uncertainty estimates. Imagining placing the midpoint of these confidence intervals at the value of each trend, and determining if there is overlap, will give a sense of whether there are statistically significant differences within groups of trend estimates.

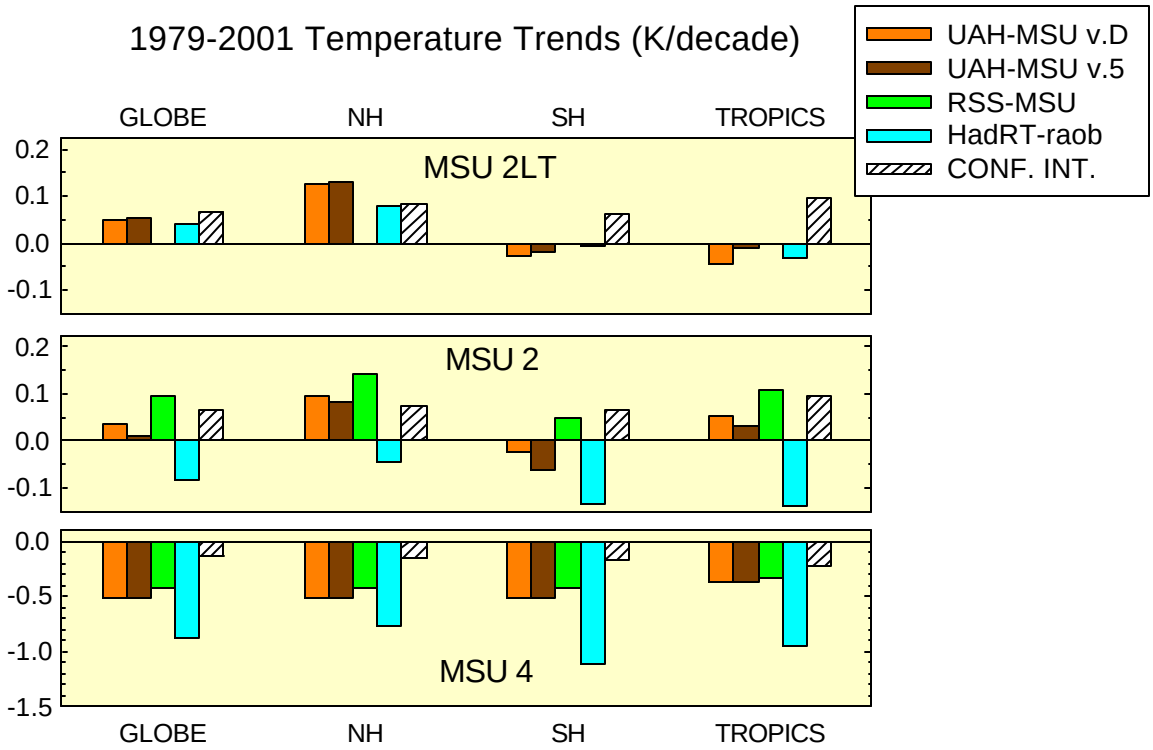

Figure 8. Trends in global temperature for 1979-2001 for three vertical layers, in four regions, from satellite and radiosonde datasets. The confidence intervals shown are typical values of the ±2 sigma uncertainty estimates. Imagining placing the midpoint of these confidence intervals at the value of each trend, and determining if there is overlap, will give a sense of whether there are statistically significant differences within groups of trend estimates.

Table 1. Correlations among global radiosonde temperature anomaly time series for 1958-1997 in three layers.

850-300 hPa	Angell-63	Angell-54	HadRT	LKS	RIHMI
Angell-63	1	.95	.81	.78	.86
Angell-54	.95	1	.79	.76	.80
HadRT	.81	.79	1	.67	.72
LKS	.78	.76	.67	1	.85
RIHMI	.86	.80	.72	.85	1

300-100 hPa	Angell-63	Angell-54	HadRT	LKS
Angell-63	1	.88	.68	.52
Angell-54	.88	1	.66	.62
HadRT	.68	.66	1	.62
LKS	.52	.62	.62	1

100-50 hPa	Angell-63	Angell-54	HadRT	LKS	RIHMI
Angell-63	1	.94	.87	.86	.88
Angell-54	.94	1	.81	.81	.82
HadRT	.87	.81	1	.87	.91
LKS	.86	.81	.87	1	.89
RIHMI	.88	.82	.91	.89	1

Table 2. Correlations among global satellite and radiosonde temperature anomaly time series for 1979-1997 in three layers.

MSU-4	UAH (ver.D and ver.5)	RSS	HadRT	LKS	
UAH	1	.98	.88	.95	
RSS	.98	1	.86	.92	
HadRT	.88	.86	1	.91	
LKS	.95	.92	.91	1	
MSU-2	UAH ver.D	UAH ver.5	RSS	HadRT	LKS
UAH ver.D	1	1.00	.93	.55	.85
UAH ver.5	1.00	1	.92	.57	.85
RSS	.93	.92	1	.45	.80
HadRT	.55	.57	.45	1	.58
LKS	.85	.85	.80	.58	1
MSU-2LT	UAH ver.D	UAH ver.5	HadRT	LKS	
UAH ver.D	1	1.00	.56	.78	
UAH ver.5	100	1	.56	.78	
HadRT	.56	.56	1	.44	
LKS	.78	.78	.44	1	

Table 3. Correlations among hemispheric satellite and radiosonde temperature anomaly time series for 1979-1997 for the MSU-2 layer.

MSU-2 N.Hem.	UAH ver.D	UAH ver.5	RSS	HadRT	LKS
UAH ver.D	1	1.00	.94	.52	.85
UAH ver.5	1.00	1	.94	.52	.85
RSS	.94	.94	1	.46	.81
HadRT	.52	.52	.46	1	.56
LKS	.85	.85	.81	.56	1
MSU-2 S. Hem.	UAH ver.D	UAH ver.5	RSS	HadRT	LKS
UAH ver.D	1	1.00	.91	.48	.77
UAH ver.5	1.00	1	.88	.45	.77
RSS	.91	.88	1	.36	.72
HadRT	.48	.45	.36	1	.41
LKS	.77	.77	.72	.41	1